Aeroelastic Stability Characteristics of an Oblique-Wing Aircraft

J. B. Crittenden* and T. A. Weisshaar†
Virginia Polytechnic Institute and State University, Blacksburg, Va.
E. H. Johnson‡
Northrop Corporation, Hawthorne, Calif.
and
M. J. Rutkowski§
U.S. Army Research and Technology Laboratory, Moffett Field, Calif.

Two different studies are presented involving a transport category aircraft with an oblique or asymmetrically swept wing. The first study concerns itself with the effect on flutter of changes in certain of the aircraft structural and inertial parameters. The second portion examines the subcritical damping characteristics of a flexible oblique-wing aircraft. For this purpose, a recent version of the NASTRAN computer code is used. A comparison is made between the flutter speeds found using the traditional *k* analysis and the results found from computation of subcritical response using the *p-k* or "British" flutter method.

Introduction

DURING the past several years, there has been a renewed interest in aircraft with obliquely swept wings. This revived interest in oblique-wing aircraft has been primarily due to the observation by Jones of the NASA Ames Research Center that, when compared to conventionally swept wings, the oblique-wing configuration provides a substantial reduction in wave drag at transonic and low supersonic speeds.[1] Further advantages have been emphasized by other studies; in particular, the variable sweep feature of the oblique-wing concept permits aerodynamically efficient operation throughout the flight envelope. For instance, the ability of the aircraft to take off and land with the wing unswept results in decreased engine noise near airports. A recent paper by Nelms[2] not only presents a thorough review of research conducted on the oblique wing, but also discusses ongoing programs. Nelms also discusses the wide range of missions, both commercial and military, for which the oblique-wing aircraft has potential applications.

Oblique-wing research has been directed primarily by the NASA Ames Research Center; this research has included extensive evaluations of the oblique-wing concept by major aircraft companies. The Boeing Commercial Aircraft Company studied a 195-passenger transport aircraft design for operating Mach numbers near 1.2.[3] The Lockheed-Georgia Company considered a 200-passenger transport (Fig. 1) designed to operate at a Mach number near 0.95.[4,5] These two efforts are cited here because they were sufficiently detailed to allow a preliminary assessment of the aeroelastic stability characteristics of their respective designs.

The antisymmetric nature of the oblique wing creates situations that cannot be readily analyzed by methods developed exclusively for bilaterally symmetric aircraft. Aeroelastic behavior is a case in point, since the aerodynamic loads and the response of the sweptforward wing segment are significantly different from those of the sweptback wing segment. Weisshaar and Ashley[6] assessed the static aeroelastic properties of the oblique wing and later related these static analysis results to dynamic stability results.[7] Significant in their findings was that the oblique wing, free to roll, had a relatively high aileron reversal speed.

Jones and Nisbet[8] considered an elementary three-degree-of-freedom analytical flutter model which demonstrated that the mode of aeroelastic instability for an oblique wing changed from static divergence to flutter when the wing was allowed rigid-body roll freedom about the fuselage centerline. This roll freedom was shown to result in a higher instability speed and to change the mode of instability as well. Through the use of sophisticated aerodynamic and structural analytical modeling, Weisshaar and Crittenden[9] confirmed the findings of Jones and Nisbet. Papadales[10] experimentally demonstrated the stabilizing influence of rigid-body roll freedom in a series of simple wind-tunnel tests at Virginia Polytechnic Institute and State University.

This paper extends the scope of previous studies by studying the effect, on aeroelastic stability, of changes in some of the structural and inertial design parameters for the

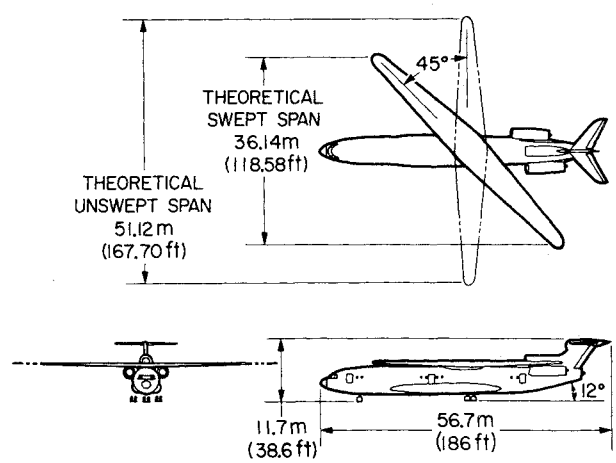

Fig. 1 Mach 0.95 oblique-wing transport.

Received March 21, 1977; presented as Paper 77-454 at the AIAA Dynamics Specialist Conference, San Diego, Calif., March 24-25, 1977; revision received March 6, 1978.

Index categories: Aeroelasticity and Hydroelasticity; Structural Dynamics; Structural Stability.

*Assistant Professor, Division of Engineering Fundamentals. Member AIAA.
†Associate Professor, Department of Aerospace and Ocean Engineering. Member AIAA.
‡Engineering Specialist, Aircraft Division. Member AIAA.
§Aerospace Engineer, Aeromechanics Laboratory. Member AIAA.

transport aircraft shown in Fig. 1. In addition, it seeks to quantify the subcritical damping behavior of oblique-wing aircraft. For this latter effort, a newly developed version of the NASTRAN computer code was used to generate aeroelastic response data. This version of NASTRAN contains a *p-k* or "British" flutter method of analysis to solve the aeroelastic response problem. These *p-k* results are compared with the results obtained using the traditional *V-g* or "American" flutter analysis method.

Effect of Parameter Changes on Aeroelastic Stability of an Oblique-Wing Aircraft

A study of the effect of some structural and inertial parameter variations on flutter of the transport shown in Fig. 1 was conducted using the classical *V-g* flutter analysis method. The wing structural idealization is taken to be a finite-element assemblage of beams whose elastic axes coincide with a theoretical wing elastic axis; these beams have plunging, pitching, and bending degrees of freedom. The wing aerodynamic loads due to oscillatory motion are described by subsonic aerodynamic influence coefficients generated by the Doublet-Lattice computer program described in Ref. 11. For a typical parameter study, angles of wing rotation or sweep are varied incrementally from 0 to 45 deg.

Figure 2 summarizes the results for two separate studies. The inertia parameter that dominates the oblique wing flutter problem has been found to be the ratio of the unswept wing roll moment of interia to the fuelage roll moment of inertia. This ratio is denoted here as I_w/I_f; for the design shown in Fig. 1 this ratio is approximately equal to 2.5. For illustrative purposes, values of I_w/I_f were chosen to be equal to 2.0 and 4.0.

To provide a basis for comparison, a stability analysis of the oblique wing with the fuselage clamped was performed first. This analysis of the clamped-fuselage aircraft determined divergence of the sweptforward wing segment to be the critical mode of aeroelastic instability. These results are displayed in Fig. 2. An increase in the wing sweep angle from the unswept position is seen to result in a decrease in divergence velocity; a minimum divergence velocity is encountered near 40 deg sweep. Thereafter, the divergence speed increases slightly. This dramatic decrease in divergence velocity with wing sweep has often been cited as the reason why an aircraft with sweptforward wings is impractical. The clamped-fuselage divergence speed provides a useful reference speed for the oblique wing, since the clamped-fuselage condition corresponds to an aircraft with a fuselage having infinite roll interia, that is, $I_w/I_f = 0$.

With fuselage roll freedom included in the analysis, two basic modes of instability are found to occur. Both modes of instability are flutter instabilities. Depending upon the sweep angle, one or the other of these modes of instability will be critical. For sweep angles of 0, 15, and 30 deg, the critical mode of instability is wing bending-torsion at a reduced frequency of approximately 0.4. This corresponds to a classical type of flutter often referred to in the literature as "fixed root" flutter.[12] As the term implies, fuselage inertia plays a secondary role in fixed-root flutter. For larger sweep angles, the critical mode of instability consists primarily of symmetric wind-bending deformation, coupled with the antisymmetric rigid-body rolling motion of the aircraft. The reduced frequency for this type of instability is typically in the vicinity of 0.04; this type of low-frequency instability is termed "body-freedom" flutter[12] because aircraft rigid-body modes of motion significantly affect the stability. The reference length used in determining both reduced frequencies is the mean aerodynamic chord for the unswept wing. The point of intersection between the two types of instability curves is indicated by a cusp, discernible in Fig. 2. As can be seen from this curve, avoidance of the body-freedom type of instability is desirable since it is associated with a substantial reduction in flutter velocities.

Figure 2 contains additional features worthy of further discussion. First of all, the fixed-root flutter velocities associated with low sweep angles are essentially unaffected by changes in fuselage roll inertia. On the other hand, the body freedom instability curve is significantly affected by changes in the roll inertia ratio. The body freedom instability curve is displaced to the right as fuselage roll inertia is decreased (or as wing roll inertia is increased). The divergence instability curve can be thought of as being the limiting case in which the fuselage roll inertia tends to infinity; conversely, as the fuselage roll inertia declines to zero the aircraft becomes a flying wing. The flutter characteristics are greatly enhanced for this latter type of aircraft. These brief studies illustrate the importance of wing sweep and the fuselage roll moment of inertia to the success of an oblique-wing design.

Similar studies including not only rigid-body roll freedom, but also rigid-body pitch and plunge reveal flutter behavior that is not much different than that found for the roll-only case. The reader is referred to Ref. 5 for a comparison of such differences.

For the stability curves presented in Fig. 2, incompressible aerodynamic theory was used for the trend studies. It is of interest, however, to obtain matched flutter speeds which account for compressibility. Figure 3 presents such a curve for

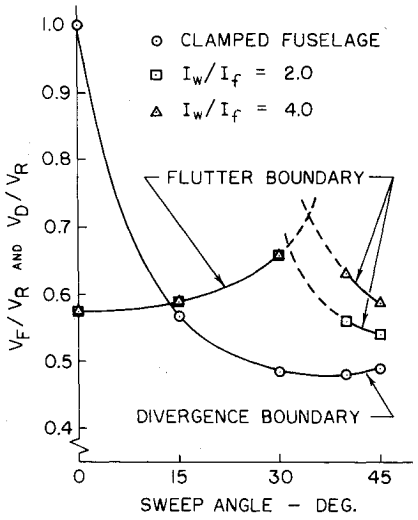

Fig. 2 The effect of sweep angle variation on roll-free flutter velocities V_F and clamped fuselage divergence velocities V_D. Results are nondimensionalized with respect to the 0 deg sweep clamped fuselage divergence velocity V_R of 447 m/s, incompressible aerodynamics, sea-level altitude.

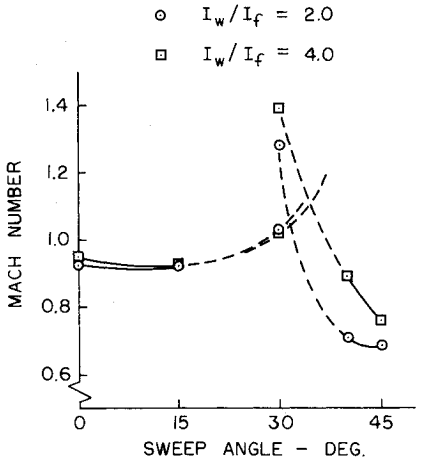

Fig. 3 Matched flutter Mach number (for $M<1$) for the roll-free aircraft, sea-level altitude.

two I_w/I_f ratios, derived using sea-level atmospheric conditions. Since subsonic aerodynamic theory was used, matching of flutter speeds is not possible for Mach numbers greater than unity. In fact, in the transonic speed regime, some serious questions may be justifiably raised. Nevertheless, the same trends shown in Fig. 2 are present in Fig. 3. At large sweep angles, the Mach number at which the aircraft may be safely operated is substantially lower than those speeds associated with low sweep angles. Because of the beneficial effect of increased altitude, the transport design was found to possess a satisfactory flutter margin at its design speed and altitude.

For the previous analyses, the elastic axis was considered to be at a nominal 38.5% wing chord location; the chordwise center of gravity position was considered to be at the 45% wing chord position. Studies of three wing center-of-gravity locations were also considered and are summarized in Fig. 4. For these studies, rigid-body plunge, pitch, and roll degrees of freedom for the aircraft were included. When fixed-root flutter is critical, a forward movement of the center of gravity causes a definite improvement in the flutter behavior as one might expect, since this is a characteristic of bilaterally symmetric aircraft. The results for the case of body-freedom flutter are found to be different. A wing center-of-gravity location of 35% gives most favorable results for 45 deg sweep, but the 55% center of gravity case appears more favorable than the 45% center of gravity case. In all cases, body-freedom flutter is undesirable at moderate sweep angles since it leads to low flutter speeds.

For an aircraft that is geometrically antisymmetric with respect to its roll axis, an immediate point of interest is the effect of using a structurally unsymmetric wing to increase fixed-root or body-freedom flutter velocities. A simple "wing tailoring" analysis was conducted to determine effects of increasing the bending and/or torsional stiffness of either the sweptforward or sweptback wing. Results of this analysis are indicated in Fig. 5.

From Fig. 5, it is seen that increasing the bending stiffness of the sweptforward wing by 20% has little effect on the fixed-root velocities, but the body-freedom flutter velocities are increased approximately 10%. Since the body-freedom flutter velocities at moderate sweep angles are relatively low, this change in the bending stiffness of the sweptforward wing allows a major enlargement in the overall flight envelope. Increasing the torsional stiffness of the sweptback wing by 20% has little effect on the body-freedom flutter velocities, but does lead to an increase in the fixed-root flutter velocities, most significantly at the larger angles of sweep. Since these fixed-root velocities are usually greater than the body-freedom flutter velocities occurring at larger sweep angles, an increase in torsional stiffness of the sweptback wing offers no major advantage. Increasing both the bending and torsional stiffness of only the sweptforward wing by 20% only improves the body-freedom flutter velocities, but not to the same extent as increasing only the bending stiffness. Thus, this change in both stiffnesses is not as beneficial as increasing only the bending stiffness of the sweptforward wing. Since the body-freedom type of flutter occurs at velocities lower than the fixed-root type at moderate sweep angles, it appears from these brief studies that increasing only the bending stiffness of the sweptforward wing will be most advantageous. These results are also consistent with the fact that the flutter speed should vary approximately as the square root of the bending stiffness. The use of differential wing stiffness appears to be an area for further study, since increases in flutter speed can be achieved by adding structural weight to only one wing segment.

The studies presented above, together with those presented in Ref. 5, clearly show that the oblique-wing aircraft is viable from an aeroelastic stability standpoint. The studies clearly show that the spanwise inertial distribution of the wing is important, as is the stiffness of the sweptforward wing. Equal in importance to the speed at which instability occurs is the subcritical aeroelastic response. It is this subject to which attention is now directed.

Subcritical Aeroelastic Response

An aeroelastic analysis package is contained in the MacNeal-Schwendler Corporation's NASTRAN program (MSC-V35).[13] The application of this capability to the oblique-wing transport configuration previously discussed can be used to evaluate the techniques used for aeroelastic stability analysis by this version of NASTRAN. In particular, the present discussion focuses on two methods of solving the complex eigenvalue problem associated with flutter analysis: an efficient form of the classical V-g or "American" method, designated as the $K-E$ method; and the $p-k$ or "British" method.

Before presenting results, it is worthwhile to review the forms of the eigenvalue problem for the two methods as they are implemented in NASTRAN. References to the two methods in the literature differ as to the precise nature of these equations. For instance, Refs. 14 and 15 both contain methods that have been labeled as either the $p-k$ or the British method but which differ slightly from each other and from the form of the $p-k$ method discussed below.

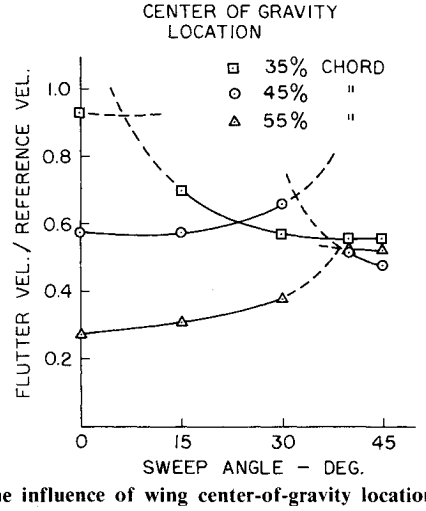

Fig. 4 The influence of wing center-of-gravity location on flutter velocities (plunge, pitch, and roll rigid-body degrees of freedom are included), incompressible aerodynamics, sea-level altitude, reference velocity = 447 m/s.

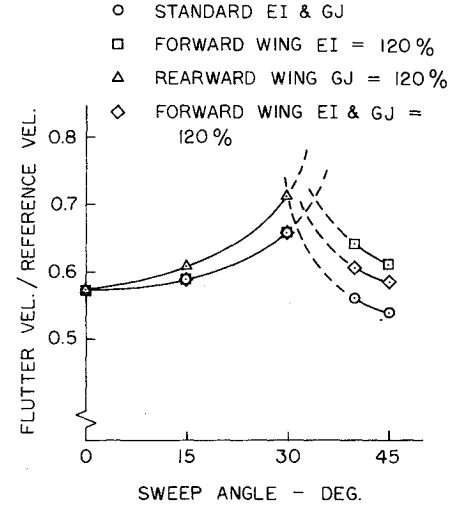

Fig. 5 Wing tailoring comparisons, incompressible aerodynamics, sea-level altitude, reference velocity = 447m/s.

Both methods start from a matrix equation given by

$$[M]\{\ddot{q}\} + [K]\{q\} - \tfrac{1}{2}\rho V^2 [Q]\{q\} = \{0\} \qquad (1)$$

where M, K, and Q are elements of the generalized mass, stiffness, and aerodynamic matrices, respectively; $\{q\}$ is a vector of generalized coordinates; and $\frac{1}{2}\rho V^2$ is the dynamic pressure. The equations contained in the NASTRAN program are more general than this, but Eq. (1) suffices for this presentation.

For the $K-E$ method, the following assumptions are made:

1) An aritificial damping term, g, is introduced by multiplying the stiffness matrix by the complex scalar $(1+ig)$.

2) The motion is assumed to be simple harmonic, i.e.,

$$\{q\} = \{\bar{q}\}e^{i\omega t}$$

Equation (1) may then be written as

$$\left[\left\{\left(\frac{2k}{\bar{c}}\right)^2 [M] + \frac{\rho}{2}[Q]\right\}\left(\frac{-V^2}{1+ig}\right) + [K]\right]\{q\} = \{0\} \qquad (2)$$

where $\bar{c}$ is a reference chord and k is the reduced frequency $\omega\bar{c}/2V$. With this formulation, the unknown eigenvalue, $\{-V^2/(1+ig)\}$, can be determined for a series of k values. Results from this determination can then be plotted in the familiar V-g format.[16]

The $p-k$ method assumes a response of the form $\{\bar{q}\}e^{pt}$, where p is a complex number. No artificial damping is included for this method as is done for the $K-E$ method. However, the imaginary part of the aerodynamic matrix is multiplied arbitrarily by p/ω.

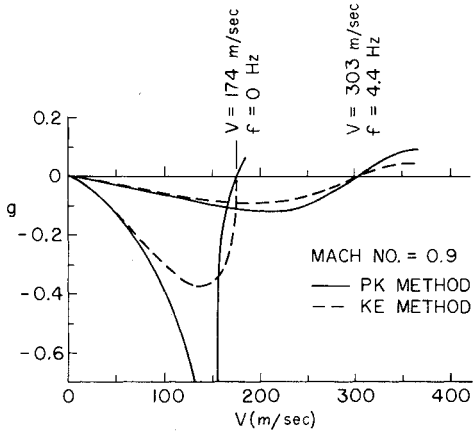

Fig. 6 Subsonic oblique wing, 45 deg sweep, clamped fuselage.

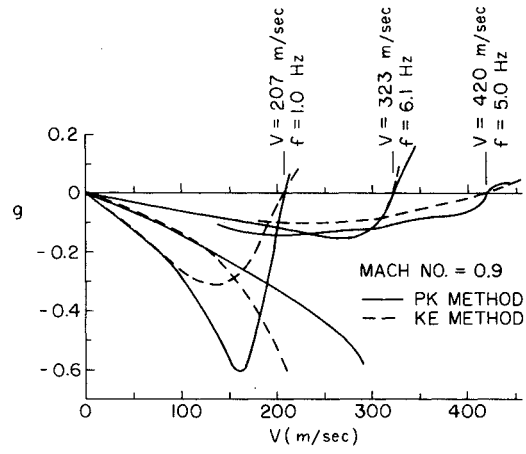

Fig. 7 Subsonic oblique wing, 45 deg sweep, free to roll, pitch, and plunge.

The aerodynamic forces are rewritten in the form

$$\tfrac{1}{2}\rho V^2 [Q] = \tfrac{1}{2}\rho V^2 [Q^R] + \frac{1}{4}\frac{\rho\bar{c}V}{k}[Q^I]p \qquad (3)$$

where Q^R and Q^I are the real and imaginary parts of Q, respectively. Equation (1) then becomes

$$\left([M]p^2 - \frac{1}{4}\frac{\rho\bar{c}V}{k}[Q^I]p + [K] - \tfrac{1}{2}\rho V^2 [Q^R]\right)\{\bar{q}\} = \{0\} \qquad (4)$$

This equation is solved by first specifying V and then iteratively solving the equations until a solution is found for which p and k are consistent. After this has been done for sufficient number of V's, curves of damping versus velocity can be plotted for this method. Rodden and Harder present a more detailed description of this method in Ref. 17.

Because the $p-k$ method does not require the inclusion of artificial damping and because it partially accounts for non-oscillatory behavior, it is felt that the method does a better job of predicting subcritical behavior. The $K-E$ method of solution is more direct and is therefore less expensive to use. The two methods predict the same instability speeds.

Results obtained using the two methods are presented in a $V-g$ format in Figs. 6 and 7. For the $p-k$ method, p is a complex number equal to $\omega(g/2+i)$. An examination of these two figures reveals agreement with the results presented in the previous section. In most respects, the two methods give similar results. A significant difference does occur in the divergence branch of Fig. 6. Referring to this figure, the branch predicted by the $K-E$ method approaches the $g=0$ axis perpendicularly but does not cross it. The corresponding $p-k$ curve is seen to attain high damping values and then return to the moderate values, before actually crossing the $g=0$ axis with a positive slope.

A more meaningful contrast of the two methods is given by Fig. 8, which plots the two divergence branches described above in a "root locus" type of format. For the $p-k$ method, the real and imaginary parts of p are plotted. The results from the $K-E$ method are plotted as a locus that has (as a function of k) ω as its imaginary part and its angle derived from the expression $g/2 = \sin\theta$, with θ measured in a counterclockwise direction from the imaginary axis. Plotting the results in this fashion shows that the $p-k$ locus first intersects the real axis and then travels along the real axis through the origin into the right half-plane. The origin in this plot corresponds to the aeroelastic divergence condition. For the $K-E$ method, the locus is seen to approach the origin with a finite imaginary

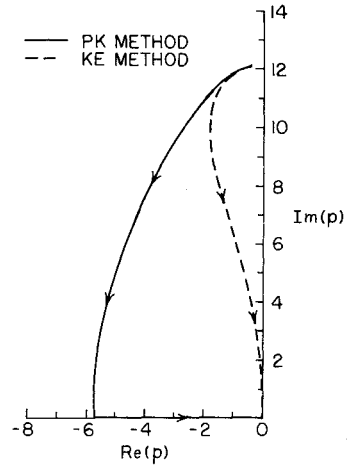

Fig. 8 Root locus for $p-k$ and $K-E$ results, oblique wing, 45 deg sweep. (Arrows indicate direction of increasing airspeed.)

part. It is also seen that this locus does not continue after the origin is reached.

A mathematical explanation for this contrasting behavior can be obtained by examining Eqs. (2) and (4) at zero reduced frequency. For this case, it is seen that Eq. (2) reduces to the equation for aeroelastic divergence, since the terms involving the mass become zero. Equation (4), at zero reduced frequency, may be written as

$$([M]p^2 - \tfrac{1}{2}\rho V^2[Q^R] + [K])\{\bar{q}\} = \{0\} \tag{5}$$

where $[Q^I]$ is zero for nonoscillatory motion. Equation (5) allows for solutions for a range of velocity values; this accounts for the travel of the $p-k$ locus along the real axis.

A physical interpretation of the two results can be found by considering a sweptforward wing in an airstream with its root fully constrained. The $K-E$ method predicts subscritical behavior, given a finite disturbance, of a damped oscillatory response. As the critical speed is approached, the frequency of the oscillations becomes small, indicating transition to a neutrally stable situation at the critical speed. The $K-E$ method cannot predict supercritical behavior, but the clear implication is that the wing will diverge. The $p-k$ method predicts a different behavior in that, before the critical speed is reached, a nonoscillatory convergent transient response is indicated. Above the critical speed, the response is characterized by nonoscillatory divergent motion.

Since both methods predict the same critical speed, one might think that the consideration of the proper subcritical behavior is academic. Furthermore, the aerodynamic forces that have been used in the model are strictly applicable only on the imaginary axis so that neither method can be expected to give exact quantitive results. In the absence of empirical information, it is impossible to say with certainty which method better predicts the subcritical behavior. However, since the $p-k$ method can approximate nonoscillatory behavior and the $K-E$ method cannot, the implication is that the $p-k$ approach is to be preferred.

This study is felt to be of value in several respects. First, the aeroelastician can always profit from a better understanding of his techniques. In addition, there are a number of situations where a knowledge of the subcritical behavior of an aeroelastic system is valuable. An important instance is in wind tunnel or flight flutter testing where it is vital to have a good estimate of the flutter boundary. Another instance, and one that is receiving increasing attention in recent years, is the integration of control systems into the aeroelastic domain. This requires aerodynamic operations that are vital throughout the left half-plane, i.e., the subcritical region.

The results given here seem to corroborate the widely held opinion that the $p-k$ method gives superior results for positively damped situations when compared to the $K-E$ method. However, there remains a need for methods that give more correct aerodynamic forces off the imaginary axis. A paper by Rodden and Stahl[18] details a method for adding transient aerodynamic influence coefficients to a strip theory analysis, and Burkhart[19] has extended this to a transient model flutter analysis using lifting surface aerodynamics. Vepa[20] treats this problem at length and provides a general method for expanding aerodynamic forces over the complete Laplace domain. Edwards et al.[21] have developed a technique for achieving the same end without introducing the additional states required by Vepa's method. Morino and Chen[22] employ a Laplace transform time solution to obtain full s (or p) plane aerodynamics for both subsonic and supersonic speeds. It is hoped that these methods will be further refined so that they can be routinely applied in aeroelastic analysis.

Finally, some mention should be made of the utility and cost of the $p-k$ method in comparison to the $K-E$ method in NASTRAN. The primary impression gained from working with this NASTRAN version is that MSC-V35 contains a tremendous aeroelastic analysis capability and should provide a basis for standardizing aeroelastic analyses. While the $p-k$ method is approximately twice as expensive to use as the $K-E$ method, this feature is compensated by the fact that $p-k$ results are easier to interpret. In addition, the subcritical predictions of the $p-k$ method are more meaningful than those found from the $K-E$ method.

Conclusions

The objectives of this paper have been twofold. First, the peculiar character of the flutter behavior of the oblique wing has been illustrated using a proposed transport aircraft design. The importance of the wing roll moment of inertia relative to the fuselage roll moment of inertia has been demonstrated. At low sweep angles, the flutter behavior tends to be similar to that of bilaterally symmetric wings. On the other hand, at moderate sweep angles, the flutter behavior tends to follow behavioral trends much like those established for sweptforward wing divergence, although the flutter speeds for this body-freedom flutter mode are significantly higher than those found for symmetric sweptforward wing divergence. An alternate method of solution for the flutter problem, the NASTRAN $p-k$ method, was also employed to demonstrate the subcritical response characteristics of this aircraft. It is demonstrated that the body-freedom instability mode is heavily damped up until the onset of flutter.

An important point that the authors would like to make is that the unsymmetrical nature of the oblique wing should be recognized and exploited in the aeroelastic design of these vehicles. In particular, the unsymmetrical arrangement of structural material should increase performance with a minimum increase in weight.

Acknowledgment

This research was supported, in part, by NASA Ames Research Center Grant NSG-2016.

References

[1] Jones, R. T., "Reduction of Wave Drag by Antisymmetric Arrangement of Wings and Bodies," *AIAA Journal*, Vol. 10, Feb. 1972, pp. 171-176.

[2] Nelms, W. P., "Applications of Oblique-Wing Technology – An Overview," AIAA Paper 76-943, AIAA Aircraft Systems and Technology Meeting, Dallas, Texas, Sept. 1976.

[3] Kulfan, R. M., et al., "Study of the Single-Body Yawed-Wing Aircraft Concept," NASA CR-137483, May 1974.

[4] Bradley, E. S., "An Analytical Study for Subsonic Oblique Wing Concept – Summary Report," NASA CR-137897, July 1976.

[5] Bradley, E. S., Honrath, J., Tomlin, K. H., Swift, G., Shumpert, P., and Warnock, W., "An Analytical Study for Subsonic Oblique Wing Transport Concept – Final Report," NASA CR-137896, July 1976.

[6] Weisshaar, T. A. and Ashley, H., "Static Aeroelasticity and the Flying Wing," *Journal of Aircraft*, Vol. 10, Oct. 1973, pp. 586-594.

[7] Weisshaar, T. A. and Ashley, H., "Static Aeroelasticity and the Flying Wing-Revisited," *Journal of Aircraft*, Vol. 11, Nov. 1974, pp. 718-720.

[8] Jones, R. T. and Nisbet, J. W., "Aeroelasticity Stability and Control of an Oblique Wing," *The Aeronautical Journal of the Royal Aeronautical Society*, Vol. 80, Aug. 1976, pp. 365-369.

[9] Weisshaar, T. A. and Crittenden, J. B., "Flutter of Asymmetrically Swept Wings," *AIAA Journal*, Vol. 14, Aug. 1976, pp. 993-994.

[10] Papadales, B. S., "An Experimental Investigation of Oblique Wing Static Aeroelastic Phenomena," Master of Science Thesis, Aerospace and Ocean Engineering Dept., Virginia Polytechnic Institute and State University, Blacksburg, Va., 1975.

[11] Giesing, J. P., Kalman, T. P., and Rodden, W. P., "Subsonic Unsteady Aerodynamics for General Configurations – Computer Program H7WC," Wright-Patterson Air Force Base, Ohio, AFFDL-TR-71-5, Part I, Vol. II, Nov. 1971.

[12] Gaukroger, D. R., "Wing Flutter," *AGARD Manual on Aeroelasticity*, Part V, Chap. 2, Feb. 1960.

[13] Rodden, W. P., Harder, R. L., and Bellinger, E. D., "Aeroelastic Addition to NASTRAN," NASA-CR to be published.

[14] Lawrence, A. J. and Jackson, J. P., "Comparison of Different Methods of Assessing the Free Oscillating Characteristics of Aeroelastic Systems," British Aeronautical Rearch Council, Current Paper No. 1084, Dec. 1968.

[15] Hassig, W. J., "An Approximate True Damping Solution of the Flutter Equation by Determinant Iteration," *Journal of Aircraft*, Vol. 8, Nov. 1971, pp. 885-889.

[16] Bisplinghoff, R. L., Ashley, H., and Halfman, R. L., *Aeroelasticity*, Addison-Wesley, Reading, Mass., 1955, pp. 566-567.

[17] Rodden, W. P. and Harder, R. L., "Flutter Analysis with Active Controls," presented at MacNeal-Schwendler NASTRAN User's Conference, Pasadnea, Calif., Jan. 1975.

[18] Rodden, W. P. and Stahl, B., "A Strip Method for Prediction of Damping in Subsonic Wind Tunnel and Flight Flutter Tests," *Journal of Aircraft*, Vol. 6, Jan.-Feb. 1969, pp. 9-17.

[19] Burkhart, T. H., "Subsonic Transient Lifting Surface Aerodynamics," *Journal of Aircraft*, Vol. 14, Jan. 1977, pp. 44-50.

[20] Vepa, R., "Finite State Modelling of Aeroelastic Systems," Ph.D. Thesis, Department of Aeronautics and Astronautics, Stanford University, May 1975.

[21] Edwards, J. V., Ashley, H., and Breakwell, J. B., "Unsteady Aerodynamics Modeling for Arbitrary Motions," AIAA Paper 77-451, AIAA Dynamics Specialist Conference, San Diego, Calif., March 1977.

[22] Morino, L. and Chen, L.-T., "Indicial Compressible Potential Aerodynamics around Complex Aircraft Configurations," Aerodynamic Analyses Requiring Advanced Computers, NASA SP-347, March 1975, pp. 1067-1110.